NANO LETTERS

LETTER

pubs.acs.org/NanoLett

Generation of Highly n-Type Titanium Oxide Using Plasma Fluorine Insertion

Hyungtak Seo,[†,‡,⊥] L. Robert Baker,[†,‡,⊥] Antoine Hervier,[†,‡] Jinwoo Kim,[§] J. L. Whitten,[∥] and Gabor A. Somorjai*[,†,‡]

[†]Chemical Sciences Division, Lawrence Berkeley National Laboratory, Berkeley, California 94720, United States

[‡]Department of Chemistry, University of California, Berkeley, California 94720, United States

[§]Department of Materials Sciences and Engineering, North Carolina State University, Raleigh, North Carolina 27695, United States

[∥]Department of Chemistry, North Carolina State University, Raleigh, North Carolina 27695, United States

Supporting Information

ABSTRACT: True n-type doping of titanium oxide without formation of midgap states would expand the use of metal oxides for charge-based devices. We demonstrate that plasma-assisted fluorine insertion passivates defect states and that fluorine acts as an n-type donor in titanium oxide. This enabled us to modify the Fermi level and transport properties of titanium oxide outside the limits of O vacancy doping. The origin of the electronic structure modification is explained by ab initio calculation.

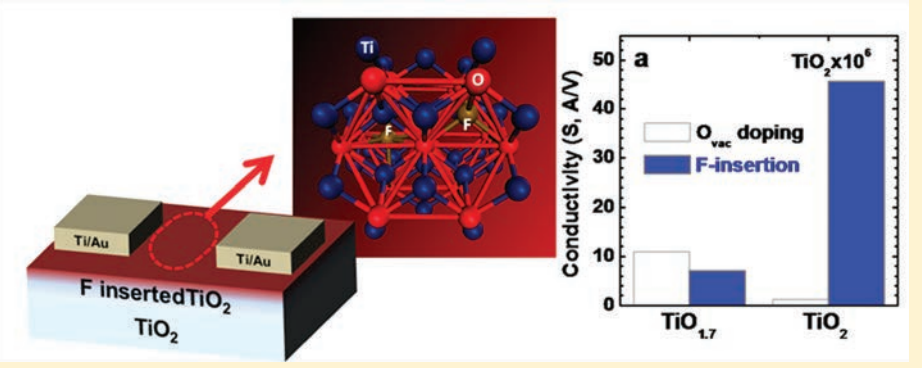

KEYWORDS: Titanium oxide, oxide doping, transport, fluorine, surface conduction

The application of transition metal oxide (TMO) semiconductors for charge-based devices is becoming prevalent for chemical, electrical, and energy applications.[1−3] Among TMOs, titanium oxide has been widely studied for photocatalysis,[4] light harvesting,[5] resistive switching memory,[6] and chemical sensing[7] as an intrinsic n-type semiconductor. The charge transport/transfer in titanium oxide is highly sensitive to O vacancy defects that exist as the lattice bonding defects in single-crystals and as surface and grain boundary defects in polycrystalline films.[8] In previous studies, O vacancies, equivalent to Ti^{3+} states, have been used as intrinsic donors to create a transport channel for increased conductivity.[9,10]

O vacancies give rise to partially occupied Ti^{3+} states below the conduction band (CB) edge and act as n-type donors. Consequently, limited control of titanium oxide conductivity and Fermi level (E_F) is possible by the manipulation of O vacancies. However, the intrinsic doping of titanium oxide through Ti^{3+} defect sites is equivalent to the formation of a reduced oxide. Although, the reduced oxide is often highly conductive, Ti^{3+} midgap states act as a barrier to CB transport and result in E_F pinning.[11] Additionally, the electric activity (e.g., charge trapping) and chemical reactivity of O vacancies create problems for material reliability. Consequently, highly conductive titanium oxide is seldom useful for device architecture, and fabrication of highly conductive, defect-free titanium oxide remains an important challenge.

The extrinsic chemical doping of titanium oxide using impurity dopants (e.g., N, S, and C) by colloidal synthesis methods to modify the electronic structure and achieve visible light absorption has been actively studied for photocatalytic applications.[12,13] Additionally, metal impurity (e.g., V, Ni, and Nb) doping to titanium oxide has been used to modify E_F and increase the conductivity.[14,15] However, in each of these cases, the semiconductor properties of titanium oxide are compromised by the formation of metallic midgap states. To the best of our knowledge, no one has reported n-type doping of a metal oxide without simultaneously decreasing the band gap. This ability would be analogous to phosphorus or arsenic doping of silicon where carrier concentration is changed without significant band structure modification.

Here we report the use of plasma-assisted fluorine (F) insertion to passivate defects and act as an extrinsic n-type donor in titanium oxide. Electrical analysis shows that F insertion is an excellent method to achieve highly conductive, low defect

Received: November 9, 2010
Revised: December 14, 2010
Published: December 22, 2010

titanium oxide suitable for TMO device applications. Theoretical calculations also investigate the concept of n-type doping to metal oxides by F insertion and suggest the mechanism by which F generates a highly conductive surface channel.

We deposited titanium oxide thin films by direct current magnetron sputtering. As deposited, these films were highly oxygen deficient. We tuned the oxygen vacancy concentration by rapid thermal annealing in O_2 at various temperatures; in this way we prepared three preconditions for F insertion with variable amounts of O vacancies. On the basis of the relative intensities of the Ti^{3+} and Ti^{4+} states in the Ti 2p XPS spectrum, we refer to the three preconditions to F insertion as $TiO_{1.7}$, $TiO_{1.9}$, and TiO_2. F insertion is achieved by treatment in N_2 plasma with trace SF_6. Process pressure was 50 mTorr with SF_6 partial pressure <5 mTorr. Plasma power is 20 W with a 130 V dc substrate bias. Treatment times ranged between 1.5 and 4.5 min.

Figure 1a shows surface conductivity measurements at room temperature for $TiO_{1.7}$ and TiO_2 before and after F insertion. In the case of $TiO_{1.7}$, the high density of suboxide states associated with the O vacancies leads to a metallic conduction (resistivity ~0.1 Ω·cm) but the conductivity decreases slightly with F insertion. This is because F passivation of O vacancies decreases the density of suboxide states used for transport in these materials. However, in the case of TiO_2, F insertion increased conductivity (i.e., decreased resistivity) by a factor of 40. Before discussing these results, it is insightful to note that for O vacancy doped TiO_X, transport occurs in the suboxide band structures induced by O vacancy defects. This is clearly evident in the activation energy of charge transport which is <0.1 eV for these samples (see Figure 1b and Supplementary Figure S1 in the Supporting Information). Polycrystalline TiO_2 will always show activation energy for CB transport of ~0.3 eV because of localized electron traps at grain boundaries.[16] We cannot measure the activation energy for transport in the TiO_2 sample because it is highly insulating. This serves to illustrate that in oxide materials true CB transport is almost impossible to observe because high conductivity in oxides is usually only achievable by reducing the O stoichiometry to create a suboxide band structure. For the F inserted TiO_2 ($F-TiO_2$) sample we observe a transport activation energy of 0.3 eV consistent with CB transport in polycrystalline TiO_2.

It is likely that this conduction is highly localized to the surface of the film. Due to the method for F insertion, we consider that F incorporates in the film primarily in the top 3 ± 1 nm as confirmed in the XPS depth profile (see Supplementary Figure S2 in the Supporting information). By acting as an n-type donor (to be discussed later) to raise E_F toward CB edge, F represents a positive space charge in the near surface region resulting in downward band bending toward the surface. If the band bending is such that the CB drops below E_F, then a shallow two-dimensional electron gas (2DEG) forms. We suggest that the 2DEG is the mechanism for the dramatic increase in conductivity for the $F-TiO_2$ sample. According to this theory, the surface channel resistivity is much lower than that shown in Figure 1a, where we conservatively consider the entire film thickness (100 nm) in determining the area of the transport channel. If the 2DEG is localized to the top 1 nm of the film as is likely, then true resistivity calculated from the device channel area could easily be 2 orders lower (~10^2 Ω·cm) than that determined by considering the entire film thickness (~10^4 Ω·cm). Note that the F appears to be stable over long periods of time. We have repeated surface conductivity measurements after storing the samples in dry N_2 for 5 months and observe no measurable loss in surface conductivity induced by F. The purpose of storing in dry N_2 is to prevent water adsorption that significantly modifies the surface electronic structure of titanium oxide.

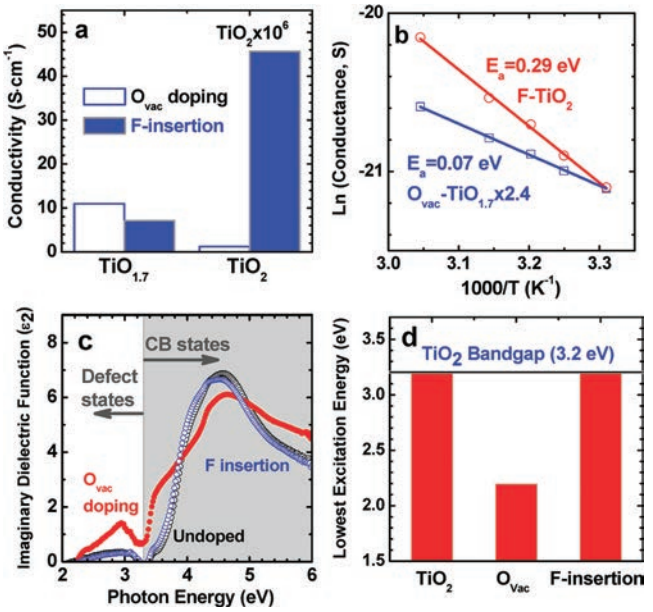

Figure 1. (a) Conductivity (S·cm^{-1}) measurements at room temperature for 100 nm TiO_X on insulating substrates. Note that the enhanced surface conductivity induced by F in TiO_2 is stable over time with no measurable loss in conductivity after 5 months. (b) Ln (conductance, S) as a function of temperature for O vacancy doped $TiO_{1.7}$ and F-inserted TiO_2 diodes. The Ln (S) values of O vacancy doped $TiO_{1.7}$ is normalized to the value of F-inserted TiO_2 at 28.7 °C (i.e., $1000/T = 3.31$ K^{-1}). The slope is proportional to the activation energy (E_a) for transport (see Supplementary Figure S1 in the Supporting Information). E_a less than 0.1 eV indicates transport in semimetal suboxide states, while E_a about 0.3 eV indicates CB transport with grain boundary defects acting as barriers. For $TiO_{1.7}$, F insertion slightly decreases conductivity by removing the suboxide states that provide the primary path for charge transport. For TiO_2, F insertion increases conductivity by a factor of 40 and shows E_a consistent with CB transport. We conclude that while F decreases suboxide transport, it produces a surface channel for enhanced CB transport. (c) Imaginary dielectric functions (ε_2) as a function of photon energy for undoped TiO_2, O vacancy doped $TiO_{1.7}$, and F inserted TiO_2 taken by spectroscopic ellipsometry measurements. CB absorption (shaded in gray) shows an onset at 3.2 eV and is nearly identical for the F inserted and undoped TiO_2 sample indicating that F insertion does not significantly modify the CB structure. At photon energies below 3.2 eV, absorption is due to O vacancy associated midgap states. (d) Lowest excitation energy of TiO_2, O vacancy doped $TiO_{1.7}$, and F inserted TiO_2 from absorption coefficient spectra (see Supplemental Figure S3 in the Supporting Information). The reference absorption onset for each excitation is ~10^5 cm^{-1}.

Figure 1c shows the photon energy dependent imaginary dielectric functions obtained by spectroscopic ellipsometry for undoped titanium oxide (i.e., TiO_2), O vacancy doped titanium oxide (i.e., $TiO_{1.7}$), and titanium oxide after F insertion (i.e $F-TiO_2$). This allows us to compare the effects of O vacancy doping and F insertion on the CB structure and minimum excitation energy. The CB edge shows an onset at 3.2 eV for TiO_2 and $F-TiO_2$ samples, indicating that F insertion does not change the band gap. Absorption at photon energies below 3.2 eV is the result of electron excitation from the valence band (VB) to midgap states associated with a suboxide band structure. By looking

dx.doi.org/10.1021/nl1039378 |*Nano Lett.* 2011, 11, 751–756

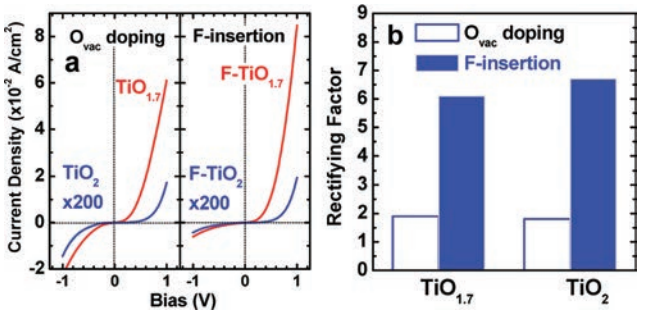

Figure 2. (a) Current−voltage (I−V) curves for ∼10 nm TiO_x on highly doped (0.01 Ω cm) p-Si. Red lines show $TiO_{1.7}$ samples, and blue lines show TiO_2. On the left is before F insertion, and on the right is after F insertion. The current density values of all TiO_2 diodes were multiplied by a factor of 200. (b) Rectifying factor for TiO_2 and $TiO_{1.7}$ before and after F doping. Rectifying factors are the ratio of forward to reverse bias current. For O vacancy doped TiO_x, low rectifying factors are the result of a high concentration of defect states and low Fermi level (E_F). By passivating defects and raising E_F, F doping increases the rectifying factor for each precondition by more than a factor of 3.

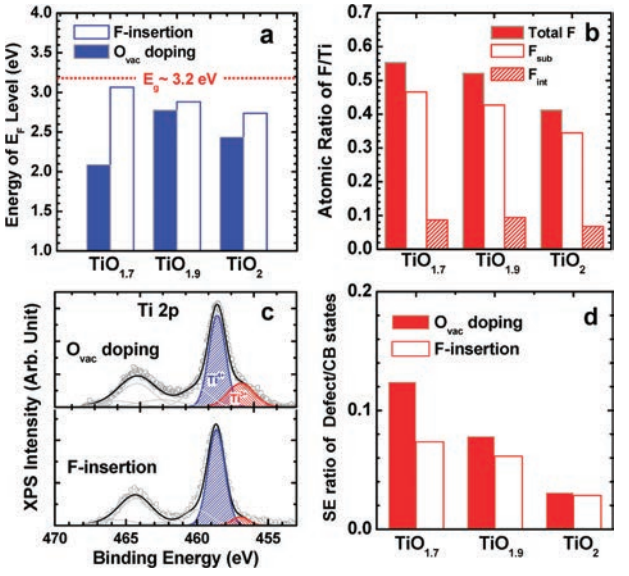

Figure 3. (a) Fermi level (E_F) before and after F insertion for each TiO_x precondition determined by fits to the valence band edge XPS spectra (see Supplementary Figure S4 in the Supporting Information). For the O vacancy doped samples, E_F is determined by Fermi pinning to O vacancy defect states. By passivating O vacancy states, F removes the effects of Fermi pinning. Additionally, F acts as an extrinsic n-type donor. As a result, F insertion raises E_F higher than is possible by O vacancy doping. For the doped samples, E_F scales with F concentration. (b) The atomic ratio of F to Ti after 3 min of plasma treatment for each TiO_x precondition. Atomic ratios are shown for two different binding states identified by XPS (see Figure 4b) and for total F. We assign these two binding states as F substituted for O and as interstitial F. Substitutional F concentration depends strongly on the initial O vacancy concentration before plasma treatment and appears to determine E_F after F insertion. (c) Ti 2p XPS spectrum of $TiO_{1.7}$ before and after F insertion. Open circles show the raw data, and lines show the results of a Gaussian deconvolution. The peak state at 458.5 eV is the Ti^{4+} state in stoichiometric TiO_2. The lower binding energy peak at 456.9 eV is the Ti^{3+} state and is a marker for O vacancy induced defect states. The decrease in Ti^{3+} state concentration with F insertion indicates that F passivates defects by binding to Ti^{3+} at O vacancies. (d) Ratio of defect state to CB absorption measured by spectroscopic ellipsometry before and after F insertion for $TiO_{1.7}$, $TiO_{1.9}$, and TiO_2. Defect state/CB absorption was taken as the maximum absorption coefficient below/above 3.2 eV. The trend shows that F passivates O vacancies that give rise to defect states.

at the relative absorption coefficients converted from the dielectric functions, it is possible to compare the density of midgap states induced by O vacancy doping and by F insertion under the joint density of states theory (see supplementary section 4 in the Supporting Information). The relative absorption of midgap states in $TiO_{1.7}$ (∼10^5 cm^{-1}) is an order of magnitude higher than that (∼10^4 cm^{-1}) of TiO_2. The lowest excitation energy for each film in Figure 1C is plotted in Figure 1D. While O vacancy doped $TiO_{1.7}$ shows the significant destabilization of intrinsic TiO_2 band structure with the low excitation energy (from top of VB to empty subgap O vacancy states) at 2.2 eV, F insertion does not induce any of change in CB edge states, stabilizing the band gap energy at 3.2 eV. As will be discussed later, this stabilized CB edge state of F−TiO_2 is due to the higher excitation energy of molecular orbital states of Ti−F bonds than 3.2 eV band gap energy of TiO_2.

Figure 2a shows current−voltage (I−V) curves for diodes consisting of TiO_x on highly doped p-Si. We present results for TiO_2 and $TiO_{1.7}$ before and after F insertion. Without F insertion, both TiO_2 and $TiO_{1.7}$ heterojunction devices show almost symmetrical I−V curves where the reverse bias leakage current is nearly as high as the forward bias current. This is the result of two factors. First, the high density of subgap states in $TiO_{1.7}$ provide a path for carrier transport in the reverse bias direction. Second, the low n-type character (i.e., low E_F level) of O vacancy doped TiO_x closely aligns with E_F in p-Si resulting in minimal interface band bending. For TiO_2 and $TiO_{1.7}$, the reverse bias current decreases and the forward bias current increases with F insertion. This is the combined effect of defect state passivation by F and increased E_F in the F−TiO_x layer to achieve greater band bending at the p-Si interface. In Figure 2b, the rectifying factor (taken as the ratio of forward to reverse bias current) increases with F insertion by a factor of 3 for both cases. A similar trend was observed for $TiO_{1.9}$ (not shown), except that the rectifying factor before F insertion was 3.4 and increased to 22.4 after F insertion. This is much higher than for TiO_2 and $TiO_{1.7}$. We do not fully understand this anomaly but believe it is in part a result of the higher E_F in $TiO_{1.9}$ before F insertion compared to either TiO_2 or $TiO_{1.7}$ as discussed below. It may seem counterintuitive that surface F doping could affect rectification at the buried Si−TiO_x interface. However, the thickness of the TiO_x layer (i.e., 10 nm) is much smaller than the depletion width. Consequently, n-type doping to the surface will still effect rectification due to the mean field across the depletion region of this p−n heterojunction.

Figure 3a shows E_F for TiO_2, $TiO_{1.9}$, and $TiO_{1.7}$ before and after F insertion. We determined E_F by fitting the valence band edge XPS spectra (see Supplementary Figure S4 in the Supporting Information). It is insightful to first consider the effect of O vacancies on the Femi level before considering the effect of F doping. In the case of stoichiometric TiO_2, we measured E_F to be 2.4 eV. Doping by O vacancies initially introduces partially occupied Ti^{3+} states about 0.3−0.5 eV below the CB edge,[17] and these states serve to pin E_F at approximately 2.8 eV in the $TiO_{1.9}$ sample. However, if the oxide is further reduced, semimetal states form that pin E_F at a much lower energy. This is evident in the $TiO_{1.7}$ sample that shows E_F to be 2.1 eV. We note that this value is in excellent agreement with the spectroscopic ellipsometry spectra that showed a minimum excitation at 2.2 eV

dx.doi.org/10.1021/nl1039378 |*Nano Lett.* 2011, 11, 751–756

(see Figure 1d). Although this reduced oxide is highly conductive, transport occurs in the metallic band structure of the suboxide, and it is not possible to use this material as a semiconductor because of the high density of midgap states.

Figure 3a also shows that F insertion raises E_F for each precondition by up to 1 eV. In the case of $TiO_{1.7}$, where E_F is initially pinned at 2.1 eV by the semimetal states of the suboxide, F insertion increases E_F to 3.1 eV, just below the CB edge. This is partly the result of F passivation of suboxides states in the band gap. However, the resulting E_F is 0.7 eV greater than undoped, stoichiometric TiO_2. We conclude that in addition to passivating defects, F acts as an n-type donor. These results demonstrate the ability of F insertion to tune E_F outside the limits of O vacancy doping. Comparing E_F after F insertion for each precondition shows that E_F scales with the atomic ratio of F to Ti determined by XPS (see Figure 3b). This indicates that F binding to an O vacancy gives rise to a free CB electron in titanium oxide. We call this effect n-type doping by F insertion. Figure 3b also indicates another binding state of F which we assign as interstitial insertion. Theoretical calculations discussed below explain the origin of these two binding states and discuss their respective contributions to modifying the bulk electronic properties. We note that E_F scales with the concentration of a F binding state at 684.9 eV that we assign as O substitution (or binding to a preexisting O vacancy).

Figure 3c shows the Ti 2p spectrum for O vacancy doped and F inserted $TiO_{1.7}$. The peak binding state at 458.5 eV is characteristic of the Ti^{4+} states in the stoichiometric oxide, while the shoulder at lower binding energy (BE, 456.9 eV) represents Ti^{3+} and Ti^{2+} states in the suboxides. Comparison of the Ti 2p spectra of $TiO_{1.7}$ before and after F insertion shows a decrease in Ti^{3+} states from 41% to 9%. This is a dramatic reduction in the density of defect states with F insertion and is direct evidence that F passivates O vacancies by binding Ti^{3+}. Figure 3D shows the absorption ratio of midgap to CB states before and after F insertion for each TiO_x precondition based on spectroscopic ellipsometry measurements. This provides additional evidence that F binding is primarily to O vacancies and that F passivates defect states in nonstoichiometric oxides. Because the chemical instability of O vacancies is one of the primary factors that limit TMO device reliability, we believe that F insertion may greatly improve the chemical stability of TMO semiconductor devices. However, we have not yet investigated the effect of F insertion on chemical stability. Note that in the case of stoichiometric TiO_2, F insertion does not significantly change the O vacancy concentration because it is already so low.

We note that SF_6 can etch TiO_2 by formation of TiF_4 which has a vapor pressure at room temperature. Fracassi et al. showed that during SF_6 plasma etching a layer of TiF_3 and TiF_4 forms on the surface of the oxide.[18] TiF_4 leaves the surface by sublimation which is likely assisted by ion sputtering in the plasma. Consequently, the formation of titanium fluorides (TiF_x) and subsequent etching represents an upper limit to F doping in TiO_2. For our plasma exposures, the F concentration stayed beneath the limit for formation of TiF_4 as can be seen by atomic fractions of F to Ti below 0.6. Fracassi et al. also showed that formation of TiF_3 and TiF_4 during etching is easily visible in the Ti 2p XPS spectrum by a 3−5 eV shift to higher BE.[19] We observe no significant shift (<0.2 eV) in the Ti 2p BE with plasma treatment. This suggests true chemical doping by F insertion rather than formation of a fluoride phase.

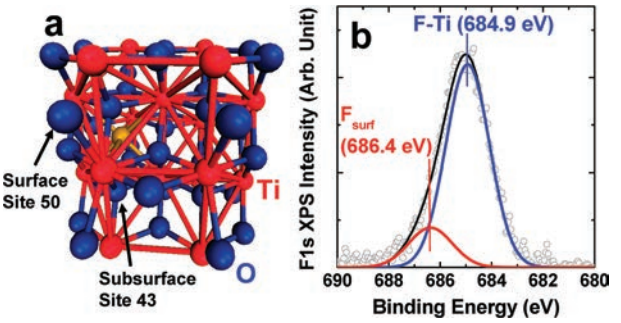

Figure 4. (a) $Ti_{18}O_{36}$ nanoparticle model with interstitial F (yellow ball) used for theoretical calculation. In this site, F sits in a distorted octahedral formed by six Ti atoms. In this case charge transfer to the F ion is primarily from a surface O atom (shown as site 50) because the nearest neighbor Ti atoms are already fully oxidized. The substitutional F site and O vacancy site (shown as site 43) have three Ti nearest neighbors. (b) F 1s XPS spectrum of TiO_2 3 min after F insertion. Open circles show the raw data, and lines show the results of a Gaussian deconvolution. The peak state at 684.9 eV indicates Ti−F bonding as a result of O subsitution. We assign the state at 686.4 eV as interstitial F. The relative energies of the two binding states are explained by the qualitatively different charge exchange between F and either Ti or O depending on the insertion site.

Theoretical calculations are carried out using a high level, many-electron theory in order to investigate fundamental properties of TiO_2. This is a well-established method for investigating the electronic structure of metal oxides.[20] The theoretical model considers three different modifications to TiO_2: (a) interstitial F, (b) F substitution for oxygen, or (c) an O vacancy. Of particular interest are effects on the electronic excitation spectrum and induced spin states that accompany changes in the occupancy of Ti d orbitals. We use a geometry optimized $Ti_{18}O_{36}$ nanoparticle to investigate these effects. While the nanoparticle differs in detail from bulk TiO_2, the interior sites involve the same basic electronic structure. Figure 4a depicts $Ti_{18}O_{36}$ nanoparticle model with an interstitial F site. In other calculations, a subsurface vacancy is created by removing a neutral O atom at the interior of the particle, and a F atom is substituted for O.

In all three systems, the lowest energy excitation is best described as exciton, with a hole that is largely localized on a single O 2p and an electron that is transferred to the d-shell of a nearest neighbor Ti. In the nanoparticle, the oxygen vacancy and interstitial F alter the excitation energy or "band gap" from the ∼3 eV of the unmodified $Ti_{18}O_{36}$. Substitutional F increases the excitation energy while an O vacancy decreases the excitation energy (see Table 1). This explains why F insertion does not alter the minimum excitation energy observed experimentally. Although F insertion creates new states in the band gap, the lowest excitation energy is still the difference between the unmodified valence and conduction band edges of stoichiometric TiO_2.

The calculations also reveal major differences in the concentration of free carrriers: an O vacancy and substitutional F induce unpaired electron spin in the d-shell of a nearest neighbor Ti, while interstitial F induces unpaired spin on nearby oxygen. One of the key findings that relates to the present investigation is the difference in behavior of subsurface species in the creation of surface electronic states involving oxygen atoms that are substantially undercoordinated, e.g., 2-fold coordinated, on the surface of TiO_2. O atoms on the surface can serve as receptors of unpaired spins generated internally and are strongly affected

dx.doi.org/10.1021/nl1039378 |*Nano Lett.* 2011, 11, 751–756

Table 1. Changes in Electronic Properties on Modification of a $Ti_{18}O_{36}$ Nanoparticle by Formation of (a) O Vacancy, (b) Substitutional F, and (c) Interstitial F

	O vacancy	substitutional F	interstitial F
increase in no. of Ti 3d electrons[a]	1.58	0.89	0.00
increase in no. of unpaired O 2p electrons[a]	0.00	0.00	0.93
F population		9.55	9.62
change in O 2p−Ti 3d excitation energy (eV)[a]	−0.3	+0.8	+0.2

[a] Changes are relative to unmodified $Ti_{18}O_{36}$.

by nearby subsurface modifications. To summarize, substitutional F is responsible for the increase of electron density in CB of TiO_2 in contrast to the increase in midgap states by O vacancy doping. Furthermore, interstitial F leads to an unpaired spin in the O 2p orbital of surface O that draws free carriers to the surface and acts as a surface conduction channel (see supplementary section 7 in the Supporting Information).

To emphasize the high level of correlation between the experimental results and the theoretical study, we briefly discuss the nature of F binding states in TiO_2 as identified by XPS spectra. Figure 4b shows the F 1s XPS spectrum for TiO_2 after F insertion. The peak is composed of two binding states centered at 684.9 and 686.4 eV. This spectrum is identical to previous reports for F insertion of TiO_2 by solution phase methods.[19] The peak state at 684.9 eV indicates Ti−F bonds by substitutional F doping. The shoulder at higher BE is a F surface state, and previous reports have hypothesized as to its exact origin.[19] We propose that the higher BE state represents interstitial F insertion (i.e., F insertion without removal of an O atom). In the case of O substitution, F coordinates to a partially oxidized Ti atom, electron density is transferred from the Ti to the F, and the Ti atom assumes a 4+ oxidation state. However, if F is inserted or bound to the surface without the removal of O, F could not draw electron density from a Ti nearest neighbor because all nearest neighbor Ti atoms are fully oxidized. In this case, the calculation suggests that F attracts electron density from a nearby O atom creating a partially unoccupied O 2p state. This is what we term interstitial insertion. The relative energies of the two binding states are explained by the qualitatively different charge exchange between F and either Ti or O depending on the insertion site.

Considering the two binding states to be equivalent to substiutional and interstitial F insertion considered by the theoretical calculations, we find excellent agreement between the theoretical conclusions and the experimental findings. First, we observe that substitutional F (i.e., binding state at 684.9 eV) scales with the O vacancy concentration before doping while interstitial F (i.e., binding state at 686.4 eV) shows little dependence on the precondition to plasma treatment. Second, we find that E_F scales closely with the concentration of substitutional F which theory predicts to generate a free electron in the Ti d shell, unlike interstitial F. Finally, the role of interstitial F to increase surface conductivity by drawing free charge carriers to the surface can explain the enhancement of surface conductivity in stoichiometric TiO_2 after F insertion. We refer the reader back to Figure 1a and 3a,b for these data.

This study demonstrates that F passivates O vacancy defects and acts as an extrinsic n-type donor for titanium oxide, resulting in greatly enhanced CB transport. This effect is stable at ambient temperature with no measurable loss of surface conductivity over several months. It is likely that F will have the same effect on other TMO semiconductors. The ability to remove midgap states and tune E_F while stabilizing the intrinsic TiO_2 band structure can result in a highly conductivity oxide suitable for device architecture and overcomes the limitations of current O vacancy doping technology for oxide semiconductors. The highly conductive surface electronic structure of n-type titanium oxide with F insertion, free of E_F level pining, is promising for many metal−oxide applications including solar cells, resistive switching memory, transparent oxide transistors, sensors, and catalysts.

■ ASSOCIATED CONTENT

Supporting Information. Details of experimental method; results of activation energy of charge transport; XPS depth profile of F-inserted TiO_x; details of SE analysis and Ti 2p, F 1s, and VB edge XPS for all TiO_x samples; and theoretical calculation details for TiO_2 with O vacancy doping and F insertion. This material is available free of charge via the Internet at http://pubs.acs.org.

■ AUTHOR INFORMATION

Corresponding Author

*E-mail: somorjai@berkeley.edu.

Author Contributions

⊥These authors contributed equally to this work.

■ ACKNOWLEDGMENT

Deposition and processing of titanium oxide films took place in the Marvell Nanolab at the University of California, Berkeley. Experimental work was funded by the Helios Solar Energy Research Center, which is supported by the Director, Office of Science, Office of Basic Energy Sciences of the U.S. Department of Energy under Contract No. DE-AC02-05CH11231. Theoretical calculations were supported by the U.S. Department of Energy, Office of Basic Energy Sciences, Division of Materials Sciences and Engineering under Award DEFG0297ER45624. H. Seo and L. R. Baker equally contributed to this work.

■ REFERENCES

(1) Wagner, J. F. *Science* **2003,** *300,* 1245–1246.
(2) Xie, X.; Li, Y.; Liu, Z. Q.; Haruta, M.; Shen, W. *Nature* **2009,** *458,* 746–249.
(3) Park, J. Y.; Lee, H.; Renzas, J. R.; Zhang, Y.; Somorjai, G. A. *Nano Lett.* **2008,** *8,* 2388–2392.
(4) Fujishima, A.; Honda, K. *Nature* **1972,** *238,* 37–38.
(5) Bach, U.; Lupo, D.; Comte, P.; Moser, J. E.; Weissörtel, F.; Salbeck, J.; Spreitzer, H.; Grätzel, M. *Nature* **1998,** *395,* 583–585.
(6) Kwon, D. H.; Kim, K. M.; Jang, J. H.; Jeon, J. M.; Lee, M. H.; Kim, G. H.; Li, X. H.; Park, G. S.; Lee, B.; Han, S.; Kim, M.; Hwang., C. S. *Nat. Nanotechnol.* **2010,** *5,* 148–153.
(7) Peng, X.; Chen, A. J . *Mater. Chem.* **2004,** *14,* 2542–2548.
(8) Valentin, C. D.; Pacchioni, G.; Selloni, A. *J. Phys. Chem. C* **2009,** *113,* 20543–20552.
(9) Zhang, Y.; Kolmakov, A.; Chretien, S.; Metiu, H.; Moskovits, M. *Nano Lett.* **2004,** *4,* 403–407.
(10) Frederikse, H. P. R. *J. Appl. Phys.* **1961,** *32,* 2211–2215.
(11) Cao, F.; Oskam, G.; Searson, P. C.; Stipkala, J. M.; Heimer, T. A.; Farzad, F.; Meyer, G. J. *J. Phys. Chem.* **1995,** *99,* 11974–11980.
(12) Asahi, R.; Morikawa, T.; Ohwaki, T.; Aoki, K.; Taga, Y. *Science* **2001,** *293,* 269–271.

(13) Chen, X.; Burda, C. *J. Am. Chem. Soc.* **2008,** *130,* 5018–5019.
(14) Choi, W.; Termin, A.; Hoffmann, M. R. *J. Phys. Chem.* **1994,** *98,* 13669–13679.
(15) Janisch, R.; Gopal, P.; Spaldin, N. A. *J. Phys.: Condens. Matter* **2005,** *17,* R657–R689.
(16) Cox, P. A. *Transition metal oxides*; Clarendon: Oxford, 1992.
(17) Lucovsky, G.; Seo, H.; Lee, S.; Fleming, L. B.; Ulrich, M. D.; Lüning, J.; Lysaght, P.; Bersuker, G. *Jpn. J. Appl. Phys.* **2007,** *46,* 1899–1909.
(18) Fracassi, E.; d'Agostino, R. *Pure Appl. Chem.* **1992,** *64,* 703–707.
(19) Czoska, A. M.; Livraghi, S.; Chiesa, M.; Giamello, E.; Agnoli, S.; Granozzi, G.; Finazzi, E.; Di Valentin, C.; Pacchioni, G. *J. Phys. Chem. C* **2008,** *112,* 8951–8956.
(20) Lucovsky, G.; Whitten, J. L. *Surf. Sci.* **2007,** *601,* 4138–4143.